



# EDC-Induced Self-Assembly of BSA-Au NCs

Wenli Zhu<sup>1</sup> · Huili Li<sup>1</sup> · Ajun Wan<sup>2</sup>

Received: 20 January 2019 / Accepted: 19 March 2019 / Published online: 15 April 2019  
© Springer Science+Business Media, LLC, part of Springer Nature 2019

## Abstract

In this paper, the Au nanoplate with bright red fluorescence was synthesized on the basis of bovine serum albumin stabilized Au nanoclusters (BSA-Au NCs). The small molecule N-ethyl-N'-(dimethylaminopropyl) carbodiimide (EDC) was used as the cross-linking agent to activate the carboxyl group on the surface of BSA, and then the condensation with amino acid in BSA induced the self-assembly of BSA-Au NCs. The particle size of Au nanoplate increased with EDC concentration. In addition, when EDC concentration was 0.0050 M, the Au nanoplate changed from smooth to grainy structure. The Au nanoplate remained the unique fluorescence characteristics of BSA-Au NCs. As EDC concentration reached 0.0025 M, the Au nanoplate even exhibited brighter red emission than that of BSA-Au NCs.

**Keywords** Au nanoplate · Fluorescence · EDC · Self-assembly · BSA-au NCs

## Introduction

The particle size of Au NCs is less than 2 nm, which is equivalent to the Fermi wavelength, resulting in the unique properties of Au NCs, such as surface plasma resonance, molecular recognition and electroluminescence [1]. By controlling the particle size and composition of Au NCs, the wavelength of photoluminescence can be adjusted in the range of visible to near-infrared light. Moreover, the Au NCs have excellent biocompatibility, fluorescence stability and nontoxicity, so there are wide application prospects in the biological analysis, imaging and therapy [2]. At present, various preparation methods of Au NCs have been developed. The thiolate, polymer, DNA and protein all can be used to synthesize the Au NCs, but there are large differences in the emission wavelength and quantum yield [3]. The Au NCs reduced and stabilized by BSA consist of 25 Au atoms.

After excitation, the BSA-Au NCs with high quantum yield (6%) can emit bright red fluorescence ( $\lambda_{\max} = 640$  nm). Due to excellent biocompatibility, high sensitivity and selectivity [4], the BSA-Au NCs have been widely used for the ion and molecule detection, bioimaging and oncotherapy [3].

The excellent performance of nanomaterials can be achieved by controlling the structure and morphology [5]. Recently, the self-assembly has been the newly-developing method to prepare the advanced nanomaterials, especially for Au nanoparticle [6]. The most typical method is template, such as surfactant, polymer and DNA and thiolic groups [7–10]. Though the remarkable developments have been achieved, there still exist problems. For example, it is difficult to control the reaction and remove the template and remnant byproduct. Lee MJ and co-workers synthesized the mesoporous gold sponges through self-assembly of citrate-covered Au nanoparticles induced by thiolated poly (ethylene glycol) [10]. For high purity, only very low concentration of thiolated poly (ethylene glycol) was mixed with the Au nanoparticles in aqueous solution at room temperature. However, the purity of as-synthesized gold sponges was 98.7%, and the residual organic molecules was removed for further purification. Li M et al. [11] also adopted thiol ligands to exchange citrate, which was the capping agent of Au nanoparticle. In the presence of 2-mercaptoethanol,

✉ Huili Li  
lihl@sjtu.edu.cn

<sup>1</sup> Engineering Research Center of Cell & Therapeutic Antibody, Ministry of Education, and School of Pharmacy, Shanghai Jiaotong University, 800 Dongchuan Road, Shanghai 200240, China

<sup>2</sup> Institute of New Rural Development, Tong Ji University, Shanghai 200092, China

the extended networks of linear and branched Au nanoparticle chains were produced only at 25–30 °C. The short-chain networks and small amounts of isolated Au nanoparticles may be produced outside the temperature range.

The small molecule-induced self-assembly using thiol and oligomer is a simple and effective method to synthesize Au nanoparticle. Wang J et al. [12] self-assembled Au nanoparticle arrays on thiol-functionalized resin beads for sensitive detection of paraquat. The Au nanoparticles also can be self-assembled by polystyrene through a combined swelling-heteroaggregation method [13, 14]. However, the other chemical reactions may occur due to the chemical activity, and the application in biology will be limited due to the bio-toxicity [15–17]. To overcome the problems, it is necessary to find a linking material with biocompatibility and unique chemical properties. As a well-known bioconjugate, EDC has higher chemical activity, and the reactivity will disappear after 1 h. Furthermore, it also possesses excellent biocompatibility and steric hindrance [18]. Lee J et al. [19] successfully obtained one-dimensional arrangement of Au nanoparticles using EDC without templates. As the carboxylate stabilizers, citrates on Au nanoparticle surfaces were activated by EDC. Then the Au nanoparticles were self-assembled to form one-nanostructure. In this paper, EDC was selected to induce the self-assembly of BSA-Au NCs. In addition, the effects of EDC concentration on the microstructure and fluorescence property were discussed.

## Experimental

BSA (66.7 kDa,  $\geq 98.0\%$ ) and chloroauric acid ( $\text{HAuCl}_4 \cdot 4\text{H}_2\text{O}$ , AR) were provided by J & K Chemical Technology. NaOH (AR) and EDC (AR) were purchased from Shanghai Lingfeng Chemical Reagent Co. Ltd. and Beijing Innochem Sci. &Tech. Co. Ltd., respectively.

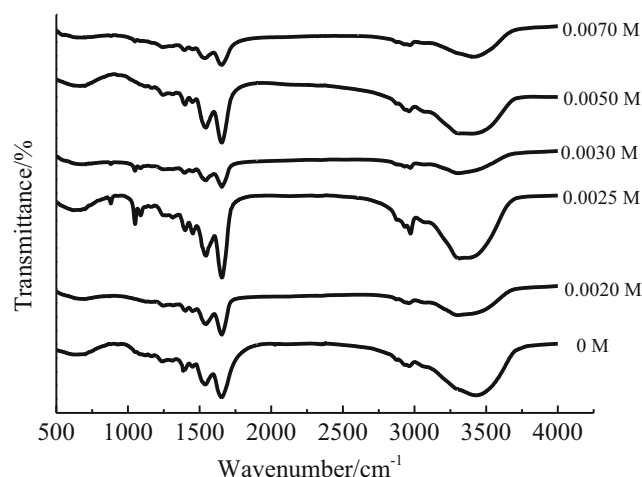


**Fig. 2** FT-IR spectra of Au nanoplate at different EDC concentrations

BSA-Au NCs were prepared according to the literature [4]. Briefly, in a typical experimental procedure, the aqueous solution of  $\text{HAuCl}_4 \cdot 4\text{H}_2\text{O}$  (10 mM, 12.5 mL) was added into the aqueous solution of BSA ( $50 \text{ mg} \cdot \text{mL}^{-1}$ , 12.5 mL) in a round bottomed flask, and stirred for 2 min to make the homogeneous precursor solution. Then the aqueous solution of NaOH (1 M, 2 mL) was introduced, and the mixture solution was incubated at 37°C for 12 h. The color of the solution changed from light yellow to light brown, and then to deep brown, which indicated the formation of the red fluorescent BSA-Au NCs. After the reaction performed for 12 h, the BSA-Au NCs were purified by dialysis against ultrapure water for 48 h using a 12 kDa molecular weight cut-off membrane. Finally, different concentrations of EDC solution ( $300 \mu\text{L}$ ) were added into BSA-Au NCs solution ( $0.025 \text{ mg} \cdot \text{mL}^{-1}$ , 20 mL). When the reaction was performed for 30 min, the products were obtained after post-treatment.

The samples were characterized by X-ray diffraction (XRD, Model D/max-2200/PC X-ray diffractometer, Rigaku Corporation, Japan) using  $\text{Cu-K}\alpha$ , Fourier transform infrared spectroscopy (FT-IR, Spectrum 100, Perkin Elmer, Inc., USA), transmission electron microscope (TEM, JEOL2010, JEOL, Japan), and luminescence spectrometer (LS 50B, Perkin Elmer, Inc., USA).

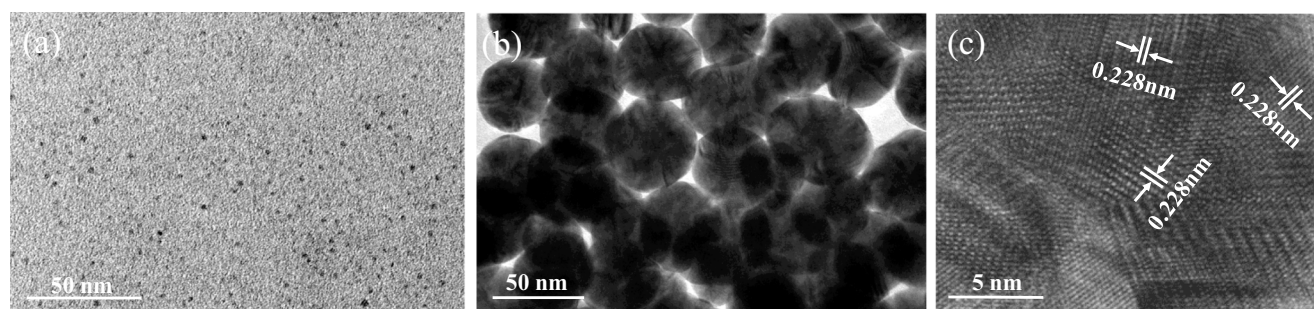


**Fig. 1** a TEM image of BSA-Au NCs, (b) and (c) TEM images of Au nanoplate at 0.0025 M EDC

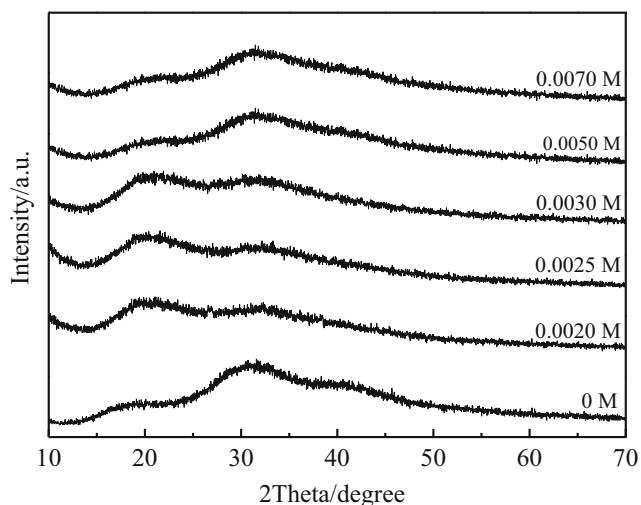


**Fig. 3** XRD patterns of Au nanoplate at different EDC concentrations

## Results and Discussion

The average particle size of obtained BSA-Au NCs is only 1.5 nm, as shown in Fig. 1a. In the presence of EDC, the BSA-Au NCs self-assemble into Au nanoplates. When EDC concentration is 0.0025 M, the Au nanoplates exhibit the quasi-wafer shape. The estimated diameter of Au nanoplate is 35–40 nm, as shown in Fig. 1b. A HRTEM image of Au nanoplate is shown in Fig. 1c. The measured fringe spacing of Au nanoplate is 0.238 nm, which is in accord well with the *d*-value of 0.236 nm for (111) plane of Au nanoparticle [20]. Therefore, it is for sure that the Au nanoplate consists of many BSA-Au NCs.

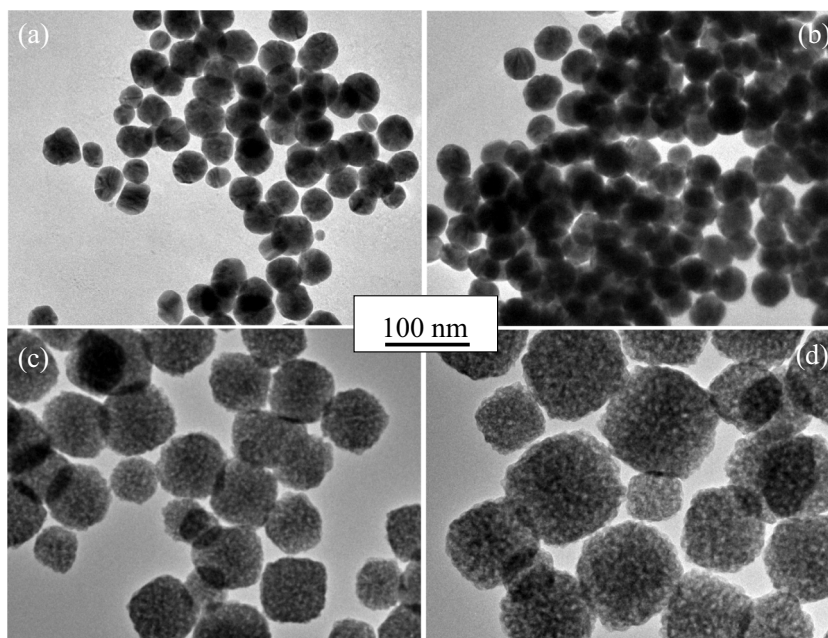
Figure 2 shows the FT-IR spectra of Au nanoplate at different EDC concentrations. When EDC concentration is 0.0025 and 0.0030 M, there appear the characteristic

absorption peaks at  $1100\text{ cm}^{-1}$ , which correspond to C-N stretching vibration of EDC. When EDC concentration increases to 0.0050 M, the absorption peaks disappear. Therefore, when EDC concentration is lower (0.0020, 0.0025 and 0.0030 M), the carbon in the imine of EDC can activate the free carboxyl group on the surface of BSA to form an intermediate, and then the condensation with amino acid in BSA induces the self-assembly of BSA-Au NCs. However, when EDC concentration is overhigh, the branched structure of Au NCs is destroyed [19].

The diffraction peak of polycrystalline Au locates at  $2\theta = 38.2, 44.4, 64.6$  and  $77.6^\circ$ , which correspond to (111), (200), (220) and (311) planes respectively [21]. As shown in Fig. 3, there is no diffraction peak belonging to Au. Thus, all peaks can be assigned to BSA. In addition, no sharp diffraction peak is observed, indicating the amorphous behavior of BSA. When EDC concentration is lower, the patterns of Au nanoplates are significantly different from BSA-Au NCs. However, as EDC concentration increases to 0.0050 M, the diffraction pattern is in accord with BSA-Au NCs. The structure change corresponds with FT-IR spectra. The reason is that the addition of EDC changes the structure of BSA.

Fig. 4 shows the TEM images of Au nanoplate at different EDC concentrations. When EDC concentration is 0.0020 M, the particle size distribution of Au nanoplate is nonuniform (Fig. 4a). As EDC concentration increases, the particle size distributes uniformly (Fig. 4b). When EDC concentration reaches 0.0050 M, the Au nanoplate changes from smooth to grainy structure, and the particle size distributes nonuniformly again, as shown in Fig. 4c and d. Additionally, it is clearly observed that Au nanoplate grows continuously with the increase in EDC concentration.

**Fig. 4** TEM images of Au nanoplate at different EDC concentrations (a: 0.0020 M, b: 0.0030 M, c: 0.0050 M, d: 0.0070 M)



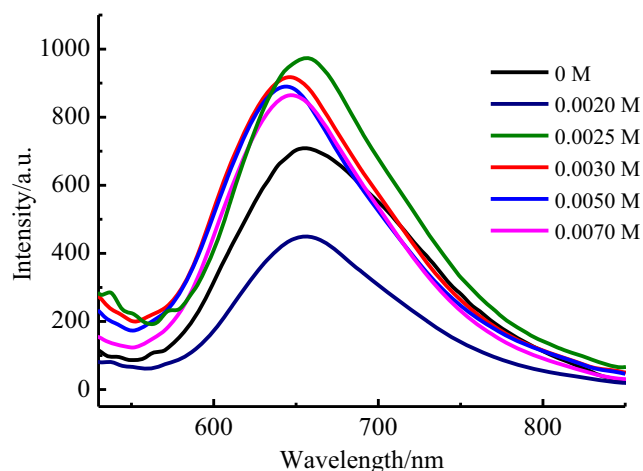


**Fig. 5** Fluorescence emission spectra of Au nanoplate at different EDC concentrations

Figure 5 shows the fluorescence emission spectra of Au nanoplate at different EDC concentrations ( $\lambda_{\text{ex}} = 470 \text{ nm}$ ). There still is obvious emission peak for Au nanoplate in the near-infrared spectral range centered at  $\sim 640 \text{ nm}$ . When EDC concentration is over  $0.0025 \text{ M}$ , the Au nanoplate exhibits brighter red emission than that of BSA-Au NCs. Moreover, when EDC concentration is  $0.0025 \text{ M}$ , the emission is the strongest.

## Conclusions

The Au nanoplate with bright red fluorescence has been synthesized by using the small molecule EDC to induce the self-assembly of BSA-Au NCs. With the increase in EDC concentration, Au nanoplate changed from smooth to grainy structure, and the particle size increased constantly. The Au nanoplate maintained the fluorescence property of BSA-Au NCs, and showed stronger emission as EDC concentration reached  $0.0025 \text{ M}$ . Moreover, when EDC concentration was  $0.0025 \text{ M}$ , the Au nanoplate exhibited the brightest red emission.

**Acknowledgements** This work was supported by the National Natural Science Foundation of China (No.21076124 and No.51173104).

## References

- Zheng J, Nicovich PR, Dickson RM (2007) Highly fluorescent noble-metal quantum dots. *Annu Rev Phys Chem* 58:409–431
- Tao Y, Li M, Ren J, Qu X (2015) Metal nanoclusters: novel probes for diagnostic and therapeutic applications. *Chem Soc Rev* 44(23):8636–8663
- Li H, Zhu W, Wan A, Liu L (2017) The mechanism and application of the protein stabilized gold nanocluster sensing system. *Analyst* 142:567–581
- Xie J, Zheng Y, Jackie YY (2009) Protein-directed synthesis of highly fluorescent gold nanoclusters. *J Am Chem Soc* 131:888–889

- Weller H (1993) Kolloidale Halbleiter-Q-Teilchen: Chemie im Übergangsbereich zwischen Festkörper und Molekül. *Angew Chem* 105:43–55
- Wang L, Wang Y, Dong S, Deng Y, Hao J (2018) Nanocapsules of magnetic Au self-assembly for DNA migration and secondary self-assembly. *ACS Appl Mater Interfaces* 10(6):5348–5357
- Xiang J, Drzal LT (2011) Electron and Phonon Transport in Au Nanoparticle Decorated Graphene Nanoplatelet Nanostructured Paper. *ACS Appl Mater Interfaces* 3:1325–1332
- Ding B, Deng Z, Yan H, Cabrini S, Zuckermann RN, Bokor J (2010) Gold nanoparticle self-similar chain structure organized by DNA origami. *J Am Chem Soc* 132:3248–3249
- Gupta P, Rajput M, Singla N, Kumar V, Lahiri D (2016) Electric field and current assisted alignment of CNT inside polymer matrix and its effects on electrical and mechanical properties. *Polymer* 89:119–127
- Lee MJ, Lim SH, Ha JM, Choi SM (2016) Green synthesis of high-purity mesoporous gold sponges using self-assembly of gold nanoparticles induced by thiolated poly(ethylene glycol). *Langmuir* 32:5937–5945
- Li M, Johnson S, Guo HT, Dujardin E, Mann S (2011) A generalized mechanism for ligand-induced dipolar assembly of plasmonic gold nanoparticle chain networks. *Adv Funct Mater* 21:851–859
- Wang J, Sun CS, Liu XF, Xin LL, Fang Y (2014) Self-assembled Au nanoparticle arrays on thiol-functionalized resin beads for sensitive detection of paraquat by surface-enhanced Raman scattering. *Colloids and Surfaces A: Physicochem Eng Aspects* 455:104–110
- Lee JH, Mahmoud MA, Sitterle V, Sitterle J, Meredith JC (2009) Facile preparation of highly-scattering metalnanoparticle-coated polymer microbeads and their surface plasmon resonance. *J Am Chem Soc* 131:5048–5049
- Lee JH, Mahmoud MA, Sitterle VB, Sitterle JJ, Meredith JC (2009) Highly scattering, surface-enhanced Raman scattering-active, metal nanoparticle-coated polymers prepared via combined swelling-heteroaggregation. *Chem Mater* 21:5654–5663
- Boal AK, Ilhan F, DeRouchey JE, Thurn-Albrecht T, Russell TP, Rotello VM (2000) Self-assembly of nanoparticles into structured spherical and network aggregates. *Nature* 404:746–748
- Hartgerink JD, Beniash E, Stupp SI (2001) Self-assembly and mineralization of peptide-amphiphile nanofibers. *Science* 294:1684–1688
- Sheng Y, Lin M, Li XW, Hao HX, Lin XY, Sun HC, Zhang H (2014) Enhancement of the 808 nm photothermal effect of gold nanorods by thiol-induced self-assembly. *Part Syst Charact* 31:788–793
- Liu TT, Chu MQ (2010) Stability of ‘quantum dot human epidermal growth factor’ bioconjugates prepared using quantum dots synthesized in aqueous solution. *J Exp Nanosci* 5:118–125
- Lee J, Zhou H, Lee J (2011) Small molecule induced self-assembly of Au nanoparticles. *J Mater Chem* 21:16935–16942
- Bian R, Wu X, Chai F, Li L, Zhang L, Wang T, Wang C, Su Z (2017) Facile preparation of fluorescent Au nanoclusters-based test papers for recyclable detection of  $\text{Hg}^{2+}$  and  $\text{Pb}^{2+}$ . *Sensors Actuators B Chem* 241:592–600
- Gluhoi AC, Bogdanchikova N, Nieuwenhuys BE (2005) The effect of different types of additives on the catalytic activity of Au/ $\text{Al}_2\text{O}_3$  in propene total oxidation: transition metal oxides and ceria. *J Catal* 229:154–162

**Publisher's Note** Springer Nature remains neutral with regard to jurisdictional claims in published maps and institutional affiliations.